Chinese Chemical Letters 35 (2024) 108438

Contents lists available at ScienceDirect

Chinese Chemical Letters

journal homepage: www.elsevier.com/locate/cclet

Benzothiadiazole-based materials for organic solar cells

Qiang Bei[a,b], Bei Zhang[a,b], Kaifeng Wang[a,b], Shiming Zhang[a,b,*], Guichuan Xing[c,*], Clément Cabanetos[d,e,*]

[a] Key Laboratory of Flexible Electronics (KLOFE) & Institute of Advanced Materials (IAM), Jiangsu National Synergetic Innovation Center for Advanced Materials (SICAM), Nanjing Tech University, Nanjing 211816, China
[b] Jiangsu Seenbom Flexible Electronics Institute Co., Ltd., Nanjing 210043, China
[c] Institute of Applied Physics and Materials Engineering, University of Macau, Macau SAR 999078, China
[d] CNRS UMR 6200, MOLTECH-Anjou, University of Angers, Angers 49045, France
[e] Building Blocks for Future Electronics Laboratory (2BFUEL), IRL2002, CNRS -Yonsei University, Seoul 03722, Republic of Korea

ARTICLE INFO

Article history:
Received 11 September 2022
Revised 30 March 2023
Accepted 7 April 2023
Available online 14 April 2023

Keywords:
Organic solar cells
Benzothiadiazole
Donor
Acceptor
Polymer
Non-fullerene acceptors

ABSTRACT

The past few years have witnessed power conversion efficiency (PCE) of organic solar cells (OSCs) skyrocketing to the value of 20% due to the outstanding advantages of organic photoactive materials. The latter, which consist of donor and acceptor materials, indeed play important roles in OSCs, and particularly one building block has attracted considerable research attention, namely benzothiadiazole (BT). The diversity of OSCs based on the BT structure have indeed sprung up, and the progressive increase in PCE values is more than just eye-catching since it heralds a renewal and bright future of OSCs. This review analyzes significant studies that have led to these remarkable progresses and focuses on the most effective BT small-molecules and BT polymers for OSC reported in the last decades. The pivotal structure–property relationships, donor–acceptor matching criteria, and morphology control approaches are gathered and discussed in this paper. Lastly, we summarize the remaining challenges and offer a personal perspective on the future advance and improvement of OSCs.

1. Introduction

Solar energy, a pollution-free, renewable, safe, and efficient green energy source, is believed to strongly contribute in solving the energy crisis of the 21st century [1–6]. Solar cells are devices, used to convert photon into electricity, can be divided into different types based on the nature of their active layer, namely inorganic solar cells [7–12], perovskite solar cells (PSCs) [13–18], and organic solar cells (OSCs) [19–24]. At present, silicon-based solar cells are developing very well (inorganic solar cells), but the preparation process is still relatively problematic, mainly from an environmental perspective (mass production and poor recyclability). OSCs have the advantages of lightweight, low price, flexibility, transparency, and large-area preparation [25–35]. They thus have broad applicative prospects in the future of building integrated photovoltaics and wearable devices. Due to an impressive and rapid development witnessed in recent years, the PCE of OSCs has now exceeded 20.2% [36]. With such a rapid growth, the field of OSC is now reviving a renewal in term of both organic active materials and devices engineering [37–39].

Even if, as mentioned PCEs have recently skyrocketing in recent years, it was in 1958 that David Kearns and Melvin Calvin used magnesium phthalocyanine as a photoactive material to prepare the world's first operating organic solar cell [40]. Then in 1986, Tang first came out with the concept of planar heterojunction organic solar cell, *i.e.*, the combination of a donor and an acceptor [41]. This device and first demonstration could reach the symbolic 1% efficiency. Significant evolution in 1995, Heeger and coworkers introduced the concept of bulk heterojunction, where both the donor and acceptor are blended to form the active layer [42]. Famous couple, the P3HT/PCBM has attracted so much research attention since promising and average power conversion efficiencies of 4% were routinely reported.

Then, Zhan and coworkers reported the star molecule ITIC, that will shortly become the new reference in academia to replace the PCBM. Devices based on blends with the high performing PTB7 successfully achieved a PCE of 6.8% [43]. Afterwards, Hou and coworkers blended ITIC derivatives with a wide-bandgap donor

* Corresponding authors.
E-mail addresses: iamsmzhang@njtech.edu.cn (S. Zhang), gcxing@umac.mo (G. Xing), clement.cabanetos@univ-angers.fr (C. Cabanetos).

https://doi.org/10.1016/j.cclet.2023.108438
1001-8417/

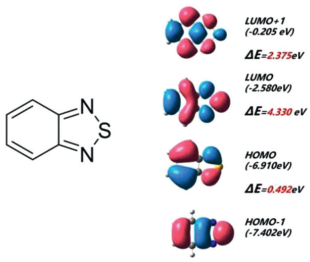

Fig. 1. DFT for BT.

polymer, namely, PBDB-T to achieve a PCE exceeding 11% with a fullerene free OSCs [44]. Later, the stacked device prepared by Chen's group achieved a remarkable PCE of 17.3% [45]. In 2019, Zou and coworkers introduced the electron-deficient unit 2,1,3-benzothiadiazole (BT) into the condensed core center to design and synthesize a new generation of non-fullerene acceptor, entitled Y6, and the single-junction device based on PM6:Y6 blend film achieved a PCE of 15.7% [46]. New standard, numerous various were reported on this new family of compound and are currently used for the preparation of record OSCs with PCEs reaching 20.2% [36].

The device of the OSCs is generally composed of transparent electrodes, photoactive materials, metal electrodes, and interface modification layers. Among them, the photoactive materials are used to absorb light to generate free electrons and holes, which will percolate to the electrodes to generate a photocurrent. Consequently, the photoactive materials are one of the most important parts of OSCs [47–50].

The OSC materials usually consist of a π-conjugated backbone constituted of electron-rich units (D) alternated with electron-deficient units (A). Developing suitable D and A unit is a reasonable solution to tune absorbing properties and facilitate efficient carrier transport to achieve higher charge mobility for the organic semiconductors and get higher PCE. Therefore, it is necessary to systematically design and synthesize novel photoactive materials which possess favorable solubility, appropriate geometry, high electron/hole mobility, and excellent optoelectronic properties [51–55]. In fact, the efforts to improve PCE in OSCs have driven the research for several years [56–66]. But there is still a lack of clear concepts and strategies to rationalize design principle and PCE. Recently, lots of the excellent donor and acceptor materials containing BT structure have been reported [67–75]. BT, which can be synthesized from *o*-phenylenediamine by reacting with sulfinyl chloride in one step [76], is used as an electron-withdrawing unit which is widely used in polymer donors (PDs), small-molecule donors (SMDs), and non-fullerene acceptors (NFAs). BT benzene constituting ring has four reactive active sites that can be substituted with either electron-donating or electron-withdrawing substituents, such as alkoxyl or halogen atoms. Of course, BT can be coupled with various conjugated units to build extended π-conjugated systems. Substitution and conjugation contribute to adjusting the frontier molecular orbitals (FMOs) of the resulting molecules [77–88]. According to the density functional theory (DFT), the high occupied molecular orbital (HOMO) energy level of BT is −6.91 eV, and the lowest unoccupied molecular orbital (LUMO) energy level of BT is −2.58 eV (Fig. 1). Therefore, in this review, we try to start with the simplest and most commonly used BT structure in OSCs to reveal the great role of such building block in photoactive materials for OSCs. In this perspective, we gather different stereo-chemical structures as well as the representative groups in the OSCs from molecular to macromolecular and donor to fullerene free acceptors.

2. BT-based small molecules for OSCs

2.1. BT-based donor molecules

BT-based donor small molecules are important contributors as active materials in OSCs. Structures of BT-based molecular donors discussed herein are depicted in Fig. 2. In 2000, the first small molecule **M1** was constructed with BT as central core, oligothiophene as linkers and triphenylamine (TPA) as the end groups. The PCE obtained was only 1.8% when blending with PC71BM, possibly due to the low charge carrier mobility and probably morphology (might show a limited solubility) [89]. The conjugation was then improved through the synthesis of the new solution-process-able organic molecule **M2** withe TPA core and BT hexylthiophene (BT-HT) arms. OSCs based on **M2**/methanofullerene [6,6]-phenyl C70-butyric acid methyl ester (C70) provided PCE of 1.96% [90]. OSC prepared from BT small molecules **M3** reached efficiencies up to 2.22% (once again with C70), which was attributed to the presence of the quinacridone solubilized with alkyl chains and light-absorbing/charge-transporting thiophene units. The absorption range and intensity were found to be well tuned by the interaction between the quinacridone core with the thiophene units [91]. Conjugated molecule **M4**, composed of a benzo[1,2-*b*:4,5-*b*′]dithiophene linked to BT units that are flanked with triphenylamine as the terminal conjugated segment, was able to reach PCE of 2.9% when blended with PC71BM and annealed at high temperature (180 °C) [92]. Molecule **M5**, where two-terminal electron-withdrawing cyanos were connected to BT, had been synthesized and used as electron donors for small-molecule OSCs. Devices based on **M5**:C70 exhibited high PCE of *ca.* 3.7% [93]. The devices based on simple molecular **M6**:C70 were characterized by open-circuit voltage (V_{OC}), short-circuit current (J_{SC}) and fill factor (FF) with V_{OC} of 0.86 V, J_{SC} of 9.89 mA/cm^2 and FF of 48%, resulting in PCE of 4.13% [94]. In 2017, asymmetric indenothiophene-core was designed to be embedded in OSCs as small-molecular donors (**M7**) for the first time. The devices prepared with PC71BM exhibited a PCE of 4.57% and a high V_{OC} of 0.98 V, demonstrating that the asymmetric indenothiophene can be an excellent donor core for small molecule semiconductors [95]. The narrow bandgap molecular **M8** was then designed and synthesized with favorable and complementary properties for light-harvesting in combination with PC71BM. (PCE of 6.7%) [96]. **M9** was prepared by combining a benzene ring with dicyanovinylene moiety and BT building block. Vacuum-deposited hybrid planar-mixed heterojunction devices utilizing **M9**/C70 active layers were able to reach promising PCE of 6.8% [97]. Efficiencies were then improved to 7.55% through the use of **M10**. The latter molecule consisted of a 5,6-difluoro-BT (DFBT) and novel asymmetry thieno[3,2-*c*]isochromene (TiC), introduced as the central electron-accepting and the electron-donating units respectively. Thiophene was used as π linker, and 1,3-indanedione as terminal unit [98].

2.2. BT-based acceptor molecules

Despite undoubtable advantages, fullerene derivatives also have several drawbacks, such as weak absorption in the visible, difficult synthesis and purification, and poor energy level tunability, hindering their large scale industrialization and further improvement of the performance of organic solar cell devices. In this context, efforts were focused in recent years to the development of NFAs. The data of BT-based donor molecules for OSCs are summarized in Table 1.

In 2007, the BT unit was first used to synthesize NFAs A0, flanked by 1-hexyl-1*H*-imidazole-4,5-dicarbonitrile (Vinazene) groups, since then, lots of NFAs with BT structure were reported **A0**-**A19** (Fig. 3) and **A20**-**A52** (Fig. 4). In OSCs based on P3HT as the

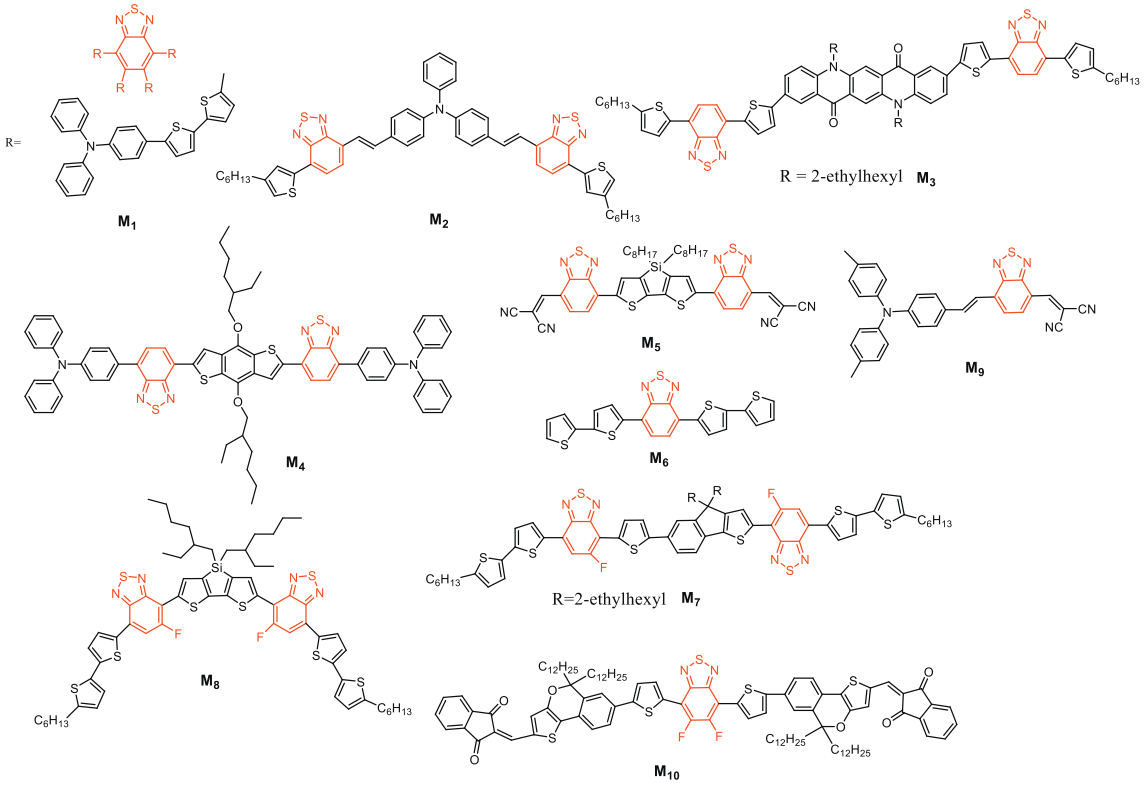

Fig. 2. BT-based donor small molecules.

Table 1
Device parameters of BT-based donor small molecules in OSCs.

	E_g^{opt} (eV)	HOMO/LUMO (eV)	V_{OC} (V)	J_{SC} (mA/cm^2)	FF (%)	PCE (%)	Acceptor	Ref.
M1	2.09	−5.40/-	0.92	4.9	41	1.80	PC71BM	[89]
M2	2.17	−5.27/−3.10	0.96	5.5	73	1.96	C70	[90]
M3	1.94	−5.55/−3.42	0.72	8.87	35	2.22	C70	[91]
M4	1.90	−5.44/−3.37	0.89	7.94	40	2.83	PC71BM	[92]
M5	1.88	−5.80/−3.92	1.05	9.79	54	3.70	C60	[93]
M6	2.20	−5.13/−3.10	0.86	9.89	48	4.13	C70	[94]
M7	1.81	−5.35/−3.56	0.98	10.24	46	4.57	PC71BM	[95]
M8	1.78	−5.12/−3.34	0.81	12.8	68	6.70	PC71BM	[96]
M9	1.86	−5.50/−3.36	0.95	15.8	55	6.80	C70	[97]
M10	1.77	−5.45/−3.26	0.90	12.63	66	7.55	PC71BM	[98]

donor polymer and **A0** as acceptor, a PCEs of 0.45% was demonstrated [99]. Sanghyuk Park and his co-workers used twisted structure of triphenylamine to build the asymmetric molecule **A1**. Devices embedding **A1**/P3HT as the active layer exhibited a maximum PCE of 0.83% [100]. Thuc-Quyen Nguyen's group reported molecule **A2** and matched it with the other donor molecule synthesized in his lab to obtain a PCE of 1.1% with all-small molecule based OSC [101]. Later, the BT unit was also combined with the diketopyrrolopyrrole (DPP) unit to further improve the PCE. For instance, Sheshanath V. Bhosale and co-works designed and synthesized molecule **A3** that exhibited a PCE of 1.16% in solution-processable photovoltaic devices once blended with the P3HT [102]. In 2012, **A4** was published with similar electron affinity than that of the standard fullerene acceptor PC60BM. However, device made with P3HT:**A4** only exhibited a PCE of 1.43%, purely due to the reduced photocurrent yield [103]. **A5** was synthesized by directly connecting BT to a phthalimides through acetylenic connectors. When blended with P3HT, **A5** based OSCs showed promising PCE of 2.05% [104]. In **A6**, the BT was combined to an imide-fused central core. Blended with P3HT, a PCE of 2.11% was achieved and devices were characterized by a relatively high V_{OC} of 0.78 V but modest J_{SC} of 6.18 mA/cm^2 and FF of 43.7% [105]. BT based molecular system **A7**, used in solution-processed non-fullerene all-molecular devices, was able to reach a PCE of 2.4% [106]. In 2011, molecule **A8** was synthesized by a combination of vinylimide and BT units, and the corresponding device showed a large V_{OC} of 0.96 V and a maximum device PCE of 2.54% in a BHJ solar cell prepared with P3HT [107]. Considering that P3HT/PCBM based devices mainly suffered of low V_{OC}, NFAs demonstrated their great potential to overcome this limitation. Conjugated molecular system **A9** was synthesized by combining naphtho[1,2-*c*:5,6-*c*′]bis[1,2,5]thiadiazole (NTz) and the fluorene-containing imide-annulated terminal units (Np). Devices based on **A9** blended with P3HT achieved a maximum PCE of 2.81%, demonstrating that the replacement of BT with NTz was a successful strategy to red-shift the absorption and fine tune the energetics by increasing the electron accepting characteristics [108]. In 2015, Won and coworkers synthesized the small molecule **A10**, composed of BT units combined with diketopyrrolopyrroles. The related devices, based on PTB7:**A10** blends, was able to reach a PCE of *ca.* 5.0% due to high J_{SC} of 12 mA/cm^2 [109]. Lim and co-workers designed molecule **A11**, achieved a PCE of 8.33% due to improved molecular packing ability [110]. In 2019,

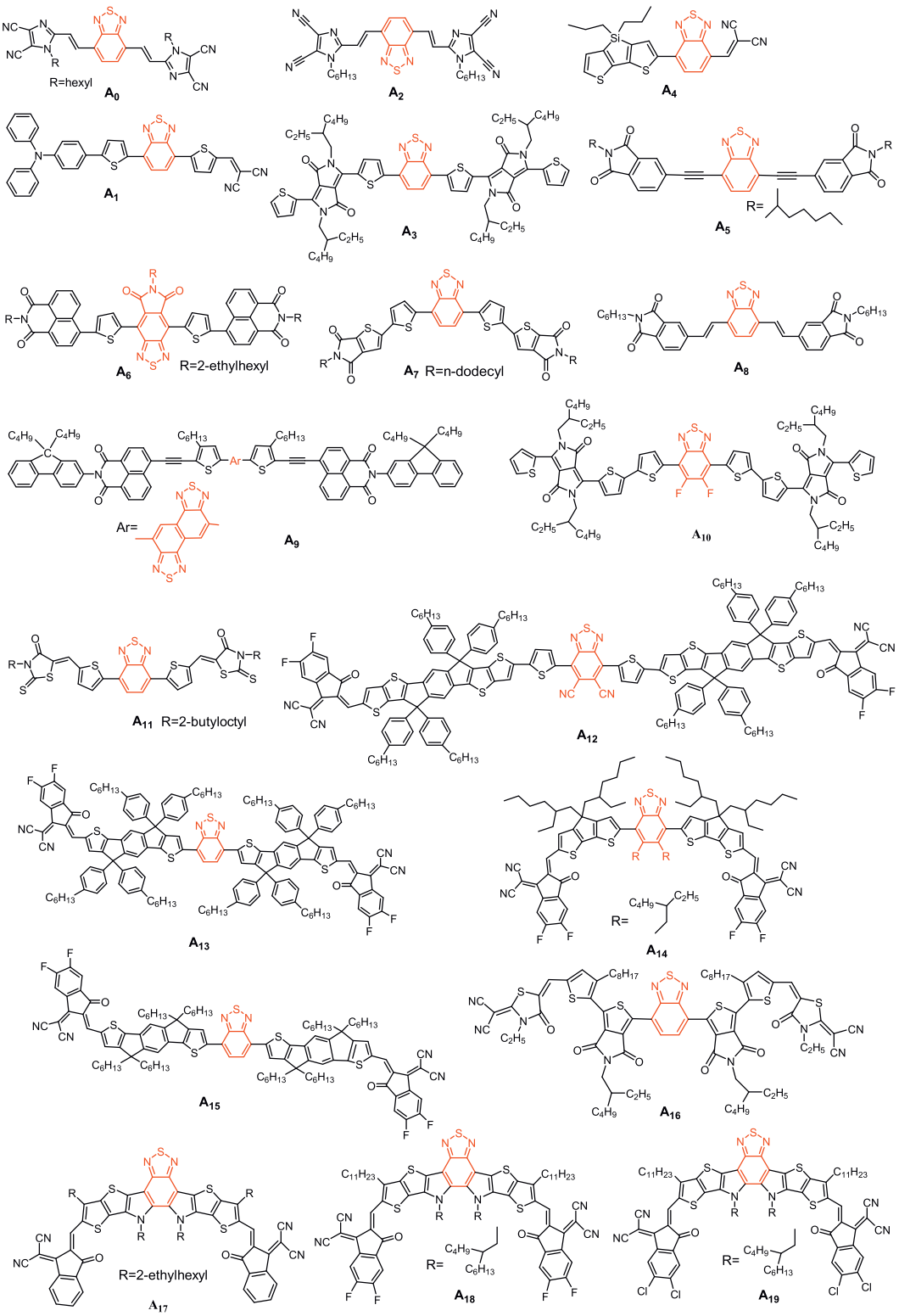

Fig. 3. BT-based acceptor small molecules **A$_0$**-**A$_{19}$**.

DoHoon and coworkers developed the molecule **A12** by introducing fluorine (F) atoms and cyano groups on 2,1,3-benzothiadiazole (DTBT). When combined with PBDB-T as donor material in small area (0.12 cm^2) inverted devices, a PCE of 9.13% was achieved [111]. Then, in 2020, Tan and co-workers explored the potential of **A13**. They replaced the 2,5-difluorobenzene (DFB) with BT, the resulting molecule **A13** exhibited better optoelectronic properties. Device-based on PBDB-T:**A13** blends achieved PCE of *ca.* 10.52% characterized by high J_{SC} of 18.59 mA/cm^2 and FF of 64.83%. These results were rationalized to the great molar absorption coefficient (1.60×10^5 L mol^{-1} cm^{-1} at 696 nm) of **A13** and multiple non-covalent conformational locks of N···S and N···H between BT and IDT unit [112]. Bo and his co-works designed and synthesized molecules **A14** using non-covalent interactions. **A14** exhibited a broad absorp-

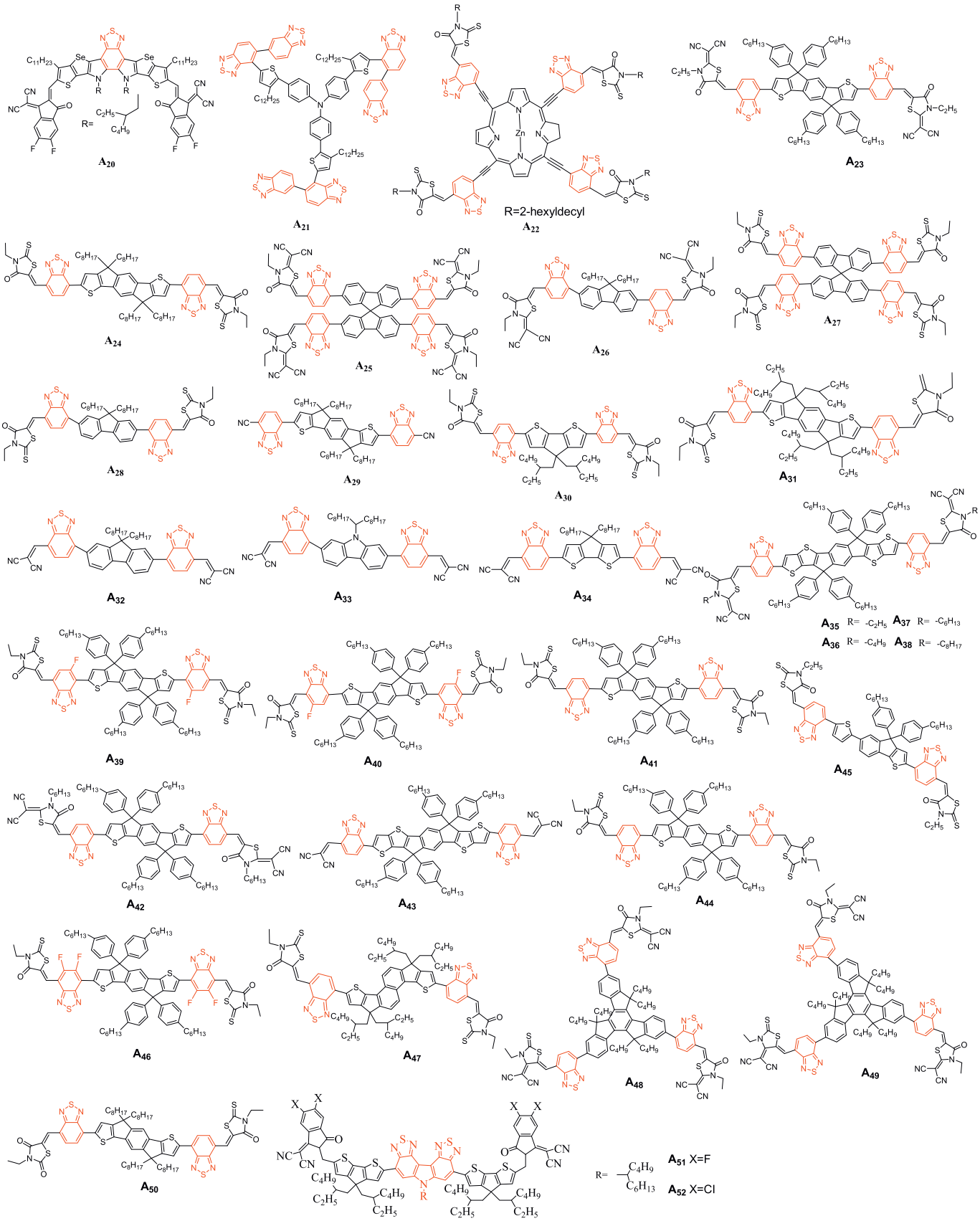

Fig. 4. BT-based acceptor small molecules **A20**-**A52**.

tion from 500 nm to 855 nm with a high molar extinction coefficient of 1.83×10^5 L mol^{-1} cm^{-1}. OSCs based on PBDB-T:**A14** achieved a PCE of 11.48%, with a low non-radiative energy loss of 0.28 eV [113]. In 2021, Zhan and coworkers, found that, through the comparison of three different central core, the BT-molecule **A15** constructed without electron bridge between the central core and moieties can lead to higher PCE (up to 11.5%) [114]. In 2020, Zhu and coworkers developed a BT based molecule (**A16**), which was used as the third component of non-fullerene ternary polymer OSCs. It turned out that incorporation of the latter molecule was beneficial to promote exciton dissociation, increase electron transport, and generally improve the crystallinity of the donor polymer (PTB7-Th). Thus, OSCs with improved PCE were achieved for the ternary (PTB7-Th: COi8DFIC:**A16**) blend compared to the binary system PTB7-Th: COi8DFIC (11.62% *vs.* 6.42% respectively) [115].

In 2019, Zou and coworkers introduced BT unit into the central core and synthesized molecule **A17** *via* the combination of dithienothiophen[3.2-*b*]-pyrrole (TPBT) and terminal 1-dicyanomethylene-3-indanone (IC). The PCEs of **A17**-based OSCs with different polymer donors (J61, PBDB-T and TTFQx-T1) were evaluated to be of *ca.* 11.0%, 13.1% and 14.1%, respectively [116]. Subsequently, fluorine atoms were introduced into the end-capped groups thus affording the well-known Y6 (**A18**). PM6:Y6-based device showed outstanding PCEs above 15% (max 15.7%). In parallel, this PCE was significantly improved by using the wide bandgap copolymer D18, since impressive PCE of 18.22% was achieved [18]. NFA **A19** incorporated chlorine atoms into end-capped groups, and once combined with PBDB-TF, a high PCE of 16.5% was achieved [119]. The selenophene[3,2-*b*]thiophene unit was introduced into the fused-ring structure to afford molecule **A20** with more obvious quinoid characteristics (Fig. 4). As a result, **A20** exhibited a higher extinction coefficient and red-shifted absorption than Y6, due to the looser electron cloud and higher polarizability of Se atom than S atom. Consequently, the PM6:**A20** devices showed a PCE of 16.02% with a V_{OC} of 0.82 V, a remarkably enhanced J_{SC} of 25.47 mA/cm^2, and a small voltage loss of 0.49 V [118].

Related studies turned to indicate that the high PCE of Y6-based devices can be attributed to the specific molecular structure of this family that can generate a large electrostatic bias potential between the donor and acceptor, which can compensate the Coulomb binding energy of the CT state. In addition, Y6 had a large fourth-order moment, which was found to be favorable for the splitting of CT states and improved the charge extraction PCE [117,120]. Several structural variations were reported to further improve the efficiencies reaching the current state of the art in this field [121–124].

On the other hand, BT was also linked/grafter to different central cores and end groups.

In 2013 Zhan and coworkers synthesized a novel star-shaped small molecule **A21** characterized by a PCE of 0.81% once blended with the P3HT [125]. Besides, Li and coworkers developed molecular **A22** through the combination of porphyrin, rhodamine and BT units. Prepared devices using the PDPP5T as donor reached a PCE of 1.9%. Even if modest, a broad photo-response from 300 nm to 850 nm, mainly due to the Soret band of the porphyrin and the intramolecular charge transfer in the molecule was demonstrated [126]. Zhou and coworkers designed and synthesized molecule **A23**. That once combined with the P3HT was able to reach a PCE of 2.55%, characterized by a decent V_{OC} of 0.72 V and FF of 61% but low J_{SC} (5.81 mA/cm^2) [127]. The same group also reported molecule **A24** where the 4-hexyl phenyl side chains of **A23** were replaced by octyl side chains. As results, **A24** showed a significant red-shift of its absorption due to better π-π stacking and stronger crystallinity. These features contributed in improving the PCEs since values up to 6.08% were achieved [128]. In 2018, Kelly and coworkers designed a two-dimensional (2D) and three dimensional (3D) BT based molecule (**A25** and **A26** respectively). Compared to **A25**, the 3D counterpart **A26** showed a higher extinction coefficient, broader absorbance bands, and a higher permittivity. In contrast, the alkyl chains of the calamitic material (**A25**) was found to facilitate the packing in solid state, significantly reduce the glass transition temperature and led to both improved electronic properties (*e.g.*, higher electron mobility) and better performance (3.3% *vs.* 1.42% for **A25** when blended with PTB7-Th) [129]. In 2019, Zhu and coworkers used a suitable donor (PffBT4T-2OD) for their molecule **A27** and successfully optimized the devices to reach PCEs of 6.15%. According to their analyses, the 3D molecular geometry of **A27** contributed in suppressing the strong intermolecular aggregation in the blend, thus leading to improved morphologies [130]. In 2014, Iain McCulloch and coworkers successfully synthesized molecule **A28** using an asymmetric BT unit. The PCE of 4.1% were achieved with P3HT which successfully exceeded those achieved with the archetypal PCBM, thus demonstrating the huge potential of NFAs [131].

Considering that the properties of the side chains have a great influence on the molecular packing, Zhang *et al.* synthesized BT based **A29** by replacing bulky side chains with simple linear alkyl chains to improve the packing ability and charge transport mobility of the molecule. A PCE of 7.3% was thus obtained for PBDB-T:**A29** based devices [132]. In 2018, Tang and coworkers synthesized the molecules **A30** by coupling a simple cyclopentadithiophene central core with two BT bridges functionalized by 3-ethylrhodanine. With 8.16% efficiencies, major assets of these devices were their stabilities, which remained at about 98% of their initial values after more than 6 months of storage [133]. With optimized morphology and obvious no evolution of the latter, this demonstration confirmed the great potential of NFAs over fullerene acceptors [134]. In this line, Peng and co-workers introduced a 3D-spirobifluorene as the central core to limit the self-aggregation of the molecule through the preparation and testing of **A31** [135]. Moreover, this phenyl based non-coplanar central core with large steric hindrance also reduced the conjugation of the molecule, resulting in a wide bandgap of 2.03 eV that was found to be particularly complementary to the PTB7-Th donor polymer. As a result, the corresponding OSCs were able to reach the symbolic 10% value (PCE = 10.12%). When the third component polymer, namely the PTB7, was added into the initial binary blend, efficiency was significantly improved to *ca.* 12.27%. Besides, Wang and coworkers synthesized a new series of NFAs composed of various electron-donating central cores namely the fluorene, carbazole, and cyclopentadiene-[2,1-*b*:3,4-*b*']dithiophene, corresponding to compounds **A32**, **A33** and **A34**, respectively. Absorption onsets gradually red-shifted from 590 nm for **A32** (590 nm), to 850 nm for **A34** through 610 nm for A33. This feature was correlated to the better conjugation and greater flatness in the case of **A34** [136]. In 2018, Holliday and coworkers reported **A34**, reaching impressive performance once blended with the wide bandgap donor P3HT (PCE of 6.4%). Definitively more efficient than the PCBM with the same polymer. Its improved air stability was also demonstrated [137]. In 2018, Qu and coworkers explored the influence of alkyl substituents on the molecular properties of 2-(1,1-dicyanomethylene)rhodanine (RCN) units. Crystal sizes in the blend films increased along the increasing number of aliphatic carbons (*i.e.*, **A35**, **A36**, **A37**, **A38**). All molecules exhibited good absorption from 600 nm to 800 nm as well as similar HOMO and LUMO energy levels. However, **A37** achieved the highest PCE (9.29%) once blended with PBDB-T. Results showed that proper adjustment of the alkyl chain on the capping group can effectively improve the charge transport properties, morphology and therefore photovoltaic performance [138]. Zhong and coworkers built molecules **A39** and **A40** differentiated by the position of a fluorine atom, *i.e.*, at the proximal end (**A40**), or at the distal end (**A39**). This subtle chemical modification of the BT structure was found to efficiently affect the optoelectronic prop-

erties. As a results, PCE of 7.5% was achieved with OSCs based on PTzBI:**A39** blends while 5.3% were reached with its counterpart under same conditions [139]. When **A39** was incorporated as the third component into the binary system composed of PBTA-BO and PC61BM, the PCE was further increased to 8.11%, due to enhanced and complementary absorption, improved open-circuit voltage, much shorter charge carrier extraction time, as well as reduced trap density and suppressed trap-assisted recombination [140].

In 2017, two ladder-type small molecule acceptors, **A41** and **A42** were embedded in non-fullerene polymer solar cells and paired with PTB7-Th to achieve a maximum PCE of 8.3% resulting from a high voltage of 1.02 V and low energy loss of 0.59 eV The reason was believed to be a beneficial effect of the post thermal annealing, triggering the local rearrangement of ladder-type molecules in the n-type phase, improving both their absorption capacity and electron transport properties and therefore increasing both the J_{SC} and FF [141]. Besides, Laquai and coworkers reported acceptor **A43** and devices prepared with PCE10 achieved a PCE of 8.4%. It was experimentally demonstrated that the reduction of both the geminate and non-geminate recombination in the blend was beneficial for the short-circuit current, and increased the energy of the interfacial charge transfer state resulting in a higher open-circuit voltage [142]. In 2017, Zhan and coworkers found that molecule **A44** could act as an energy driver to increase the driving force for charge transfer while achieving a very small energy loss (0.55 eV) in a ternary blend with PTB7-th and PDI-2DTT. A PCE of 10.1% was reported for such system [143]. In addition, Peng and coworkers developed the molecule **A45** by reducing the fused-ring core and shortening the side chains to improve both the optical and energy levels compatibilities with the PTB7-Th resulting in high EQE above 45% in the 350–700 nm range. As a result, **A45**-based device exhibited a large V_{OC} of 1.04 V and a high PCE of 8.7% with an extremely low energy loss of 0.55 eV, due to shorter side chains with better crystallinity and higher mobility of charge carriers [144]. BT based molecule **A47** was synthesized through a double fluorination strategy. Embedded in a ternary device (PBTA-BO:**A46**:PC71BM), high PCE of 9.06% was demonstrated. Compared to its mono-fluoride-substituted counterpart, HOMO and LUMO energy levels of A46 were found to be stabilized and the molecular absorption spectrum of the molecule further red-shifted [145].

In **A47**, the central benzene ring was replaced by trapezoidal dithiophenaphthalene (DTN) (Fig. 4), resulting in the destabilization of its LUMO level. Device fabricated with the PTB7-Th:**A47** blend as the active layer achieved a decent PCE of 9.51%, but high V_{OC} of *ca.* 1.08 V and a V_{loss} reduced to 0.5 V. These features were correlated to the change of the central nucleus from benzene ring to naphthalene ring that increase the conjugation length of the electron-donating unit [146]. In 2019, Wu and coworkers designed and synthesized two novel wide-bandgap NFAs, namely **A48** (2.19 eV) and **A49** (2.10 eV), with non-coplanar three-dimensional structure [147]. Both designed molecules were efficient to prevent excessive molecular aggregation (layer stacking distance of 18.8 Å and 17.9 Å, and showed π-π stacking distances of 3.90 Å and 4.00 Å, respectively). While a smaller distortion angle was measured for **A49** compared to **A48**, **A49** showed stronger crystallinity and higher carrier mobility, which was found to be beneficial for both the J_{SC} and FF. Hence, when mixed with PTB7-Th, a PCE of 10.15% and 8.29% were achieved for **A49** and **A48**, respectively [147].

In parallel, Wadsworth and his co-workers investigated the impacts of non-halogenated solvents on the performances of **A50**-based devices. When the 1,2,4-trimethylbenzene (TMB) was used as the solvent instead of chlorobenzene (CB), the PCE of PffBT4T-2DT:**A50** based devices increased from 10.2% to 11.1%. Moreover, it is noteworthy that no additives, nor thermal treatment were necessary [148]. The solubility of the polymer donor (PffBT4T-2DT) and the absorption coefficient of the mixed film treated with TMB were found to be higher than that of CB processed films. Recently, Cui and his coworkers used constructed with a novel electron-deficient block unit *N*-(2-butyloctyl)-carbazole[3,4-*c*:5,6-*c*]bis[1,2,5]thiadiazole (CBT) synthetic NFREAs **A51** and **A52** (Fig. 4), the PCE of PBDB-T:**A52** based device is 10.18% and much higher than that of PBDB-T:**A51** (7.05%), due to **A52** has a deeper energy level, stronger S···N conformation lock, a larger van der Waals surface area, and electrostatic potential (ESP) maximum value. As a result, the CBT structure with BT unit performs great potential in the construction of high-performance active layer materials of BT-OSCs [149].

For OSCs, machine learning (ML) algorithms should be introduced to replace the traditional scientific research based on trials and errors, which consumes a lot of time and cost [13]. For instance, Pereira and coworkers explored ML models to predict the HOMO and LUMO energy levels of molecules based DFT (B3LYP) and 2D structures calculations performed on more than 111,000 molecules. Accurate results within 0.15–0.16 eV of absolute error were computed for HOMO or LUMO output. Such stochastic model has great potential application for adjusting energy levels to help organic chemist for the design of new molecular structures for OSCs with high V_{OC} [150–157].

Besides, Kokate *et al.* took the morphology of the binary film as the basis of basic classification to evaluate the J_{SC} of each device, the surprising accuracy of results based on convolutional neural networks (CNN) based model reached a value of 95.8% [158]. It is also noteworthy that Su *et al.* used bis-tricyclic aromatic enes (BAE) as the basic central-design unit and employed a ML model to screen and simulate suitable acceptors to match donor materials.

Considering that ML was only recently applied in the field of OSCs, many drawbacks still remain to the wider application of such predictable method. On one hand, current ML models are still unable to describe the complex morphology, charge separation and transfer processes in OSCs mixed membranes. On the other hand, device-related test data are highly dependent on the environment, device engineering and instrumentation. In other word, with no unique and agreed way of preparing and testing the devices, so analyze, and transplantation of data into computer language is almost impossible.

3. BT-based polymers for OSCs

Polymer materials for OSCs have attracted considerable research attention due to their adjustable structure and amazing film forming properties. Over the years, BT, either functionalized by alkoxy or halogene groups, became a series of monomers for OSC polymer [159–164]. Hence, in this section, several BT based donor polymers (**P1**-**P25**) and acceptor polymers (**P26**-**P35**) were gathered and discussed on the basis of the PCE (Fig. 5).

3.1. BT polymer donor

The first BT-polymer, **P1**, consisting of the BT units co-polymerized with thiophenepyrrole-thiophene, was reported in 2001 by Janssen and coworkers. Due to the mismatch of energy levels, **P1**:PC61BM only showed a PCE of 0.34% [165]. **P2** was synthesized to match with P3HT, but the PCE based on such blend was only of *ca.* 0.02%, due to the poor solubility of the BT based polymer [166]. To improve the overall solubility, a fluorene unit with two soluble alkyl side-chains was co-polymerized with the BT in 2003 to afford polymer **P3**. As a result, PCE was significantly increased to 2.41% [167]. Besides, in 2007 [168], Brabec

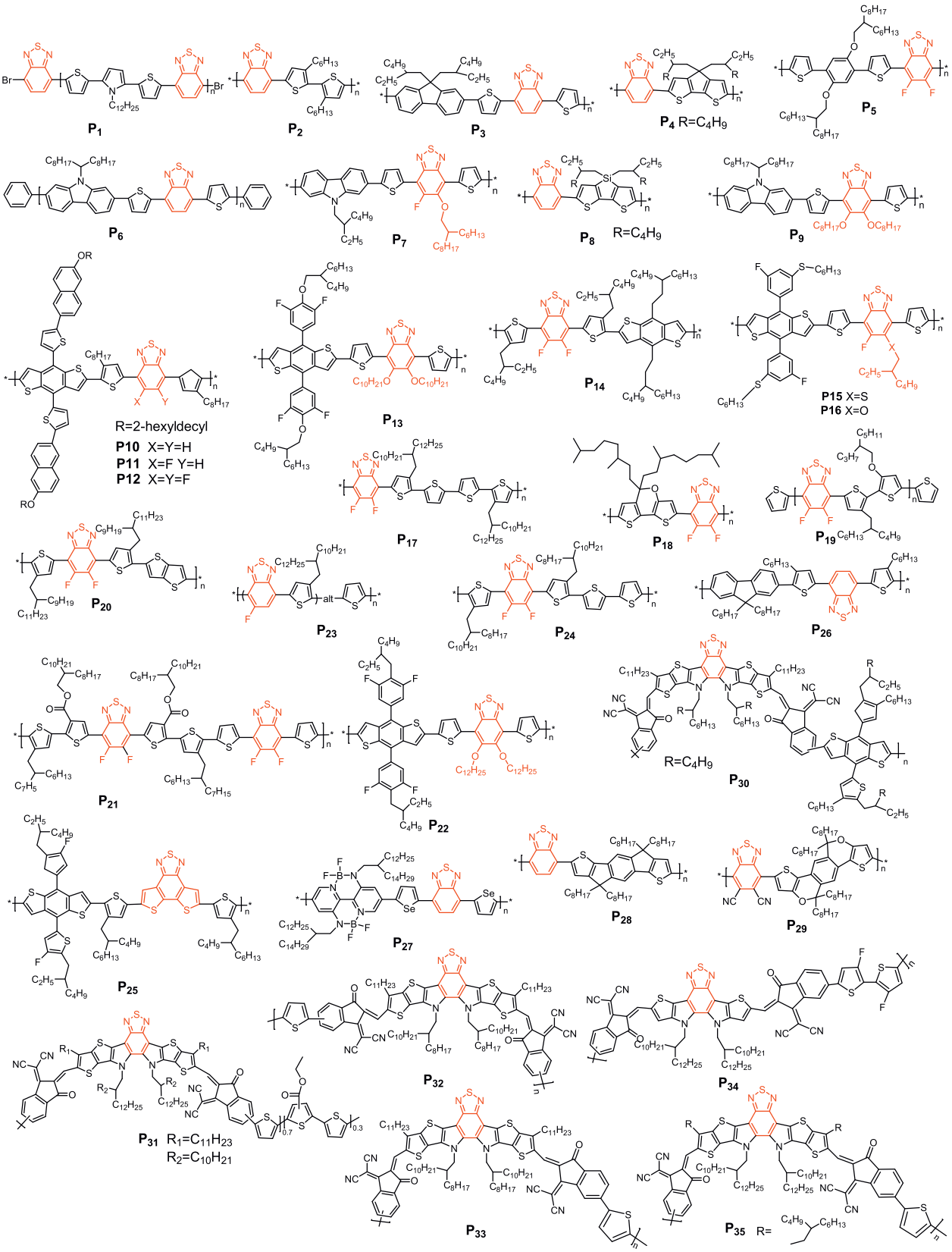

Fig. 5. BT-based polymers.

and coworkers combined BT with the cyclopentylthiophene co-monomer to afford **P4**, characterized by an improved solubility and decent hole transporting properties. The device made from a blend with PCBM were thus able to achieve a PCE of 3.5%. In 2015, Kim and coworkers synthesized **P5** (Mn = 40 kg/mol), to study the relationship between molecular weight and photovoltaic properties. After **P5** was combined with P(NDI2OD-T2), promising PCEs of 3.59% were achieved with such all polymer solar cells [169]. Besides, Leclerc and coworkers reported **P6**, a polymer based on a 2,7-carbazole and BT, that was found to improve the solubility, the planarity and conjugation within the backbone. With better optoelectronic and probably charge transport properties, PCEs were thus further improved to *ca.* 3.6% [170]. Then a PCE of 3.71% were achieved by Bo and coworkers through the preparation and use of the BT polymer **P7** as donor in combination with the Ni-based molecule NI-AA-NI. Note that despite modest efficiencies, impressive high V_{OC} of *ca.* 1.07 V were measured [171]. In 2008, Yang and coworkers synthesized the BT-polymer **P8** by introducing the silicon-contained fused bithiophene as the electron-rich co-monomer, resulting in light absorption in the near infra-red region since characterized by an onset at *ca.* 800 nm. Once blended with C70 as acceptor, a promising PCE of 5.1% was successfully achieved [172]. Then, in 2009, Bo and coworkers reported the polymer **P9** in which the BT units was functionalized with two alkoxy side chains, resulting in improved solubility and probably ideal morphology once processed with PC71BM since the successful use of additives 1,8-diiodooctane (DIO) led to a PCE of 5.4% [173]. In 2017, Kim and coworkers had reported a series of BT based polymers (**P10**, **P11** and **P12**) differentiated by the number of fluorine atoms on the BT unit [174]. They found out that the latter polymers exhibited enhanced dipole moments difference ($\Delta\mu$) between the ground and excited states upon successive addition of fluorine atoms. When combined with P(NDI2HD-T2 as the acceptor, the large $\Delta\mu$ of **P12** was found to facilitate exciton dissociation while suppressing charge recombination in the corresponding OSCs. Therefore, while device made with this polymer successfully achieved a promising PCE of 6.24%, devices prepared with its fluorene-free analogue (**P10**) reached PCE only around 3% (max 2.65%). On the other hand, Liu and coworkers also introduced different numbers of fluorine atoms into BT based polymers to tune their crystallinity and self-assembly properties. Hence, **P13**, functionalized with four fluorine atoms per monomer reached a PCE of 6.45% when blended with RR-PBN [175]. Other example of successful use of fluorine functionalized BT monomer was reported by Zhou and coworkers in the preparation of **P14**. Due to its strong electron absorption capability in the visible region, PCEs of 7.2% were thus achieved in fullerene based OSCs [176]. The versatility of the BT unit, from an organic chemistry point of view, allowed numerous structural modifications and functionalization. For instance, Bo and coworkers explored the concept of asymmetric BT monomers either functionalized by an alkoxy (**P15**) or thioalkoxy group (**P16**). It turned oud that the nature of the heteroatom strongly affected the photovoltaic performance since PCE of 7.2% were achieved with the oxygen based polymer (**P15**) while PCE of only 1.55% was reached for its sulfur analogue, namely **P16** [177]. On the other hand, to improve the overall solubility, Chen and coworkers developed, in 2014, the **P17**, by functionalizing a thiophene co-monomer on its position 3 with long branched alkyl side chains. Inverted solar cells were then prepared and PCEs of 7.64% were achieved for 230 nm thick active layers [178]. Further improvement (PCE = 7.9%) were reported in 2013, through the preparation of **P18** in which an oxygen atom was introduced into the cyclopentadithiophene (CPDT) based co-monomer [179]. A significant jump of efficiencies was then achieved by Guo and coworkers since PCEs of 9.76% were reached with devices made from **P19** and the PC71BM [180]. This symbolic step was overcome in 2018 by Yan and coworkers with **P20** that was successfully combined with the NFA entitled O-IDTBR (PCE of 10.4%) [181]. In 2016, Yan and coworkers reported a series of OSCs embedding BT-based polymers **P21** used that was combined with perylene bisimide (PBI) derivatives. Beyond the promising PCEs of 10.5%, nearly 90% of internal quantum efficiency was demonstrated despite a low voltage loss of 0.61 V [182]. A slight improvement was reported by Zhan and coworkers (11.03%) with their polymer **P22**, consisting in an alkoxy functionalized BT copolymerized with a benzodithiophene (BDT) decorated with lateral fluorobenzene units [183]. On the other hand, Huang *et al.* developed a design strategy based on random copolymer (polymer **P23**) for large-area OSCs. The device based on **P23**:IEICO-4F exhibited the promising PCE of 12.1% with active layer's thickness over 300 nm [184]. The 13.07% of PCE were then reached by Zhu and coworkers with their simple polymer **P24**, but this time blended with ZITI-N-EH [185]. Recently, Ding *et al.* prepared the BT-based donor polymer **P25** with high planarity, which was fond to be favorable for charge transport since high hole mobility of 1.59×10^{-3} cm^2 V^{-1} s^{-1} were measured. When combined with a Y6-based acceptors, impressive PCE of 18.22% were achieved in single junction fullerene free OSCs [18] (Table 2).

3.2. BT polymer acceptor

Starting in 2008, the first BT-polymer (**P26**) was used as acceptor to prepare an all-polymer OSCs with the archetypal P3HT donor polymer that were characterized by a modest PCE of 1.2% [186]. Liu and coworkers synthesized the boron containing conjugated polymers **P27**, that was successfully associated with a donor polymer based on benzo[1,2-*b*;4,5-*b*']dithiophenes and benzotriazole to achieve encouraging PCEs of *ca.* 5.37% and high V_{OC} of 1.08 V [187]. In 2020, Feng and coworkers have developed the narrow band gap BT based polymer **P28** (E_g^{opt} = 1.43 eV). Once blended with the complementary PBDB-T donor polymer, devices characterized by a broad photo-response from 300 nm to 850 nm and promising PCEs of 8.32% were successfully prepared [188]. In recent work, authors introduced a strong electron-donating co-monomer into the conjugated backbone (**P29**) to further broaden the absorption spectrum, and thus to reach a very low bandgap of 1.28 eV, resulting in a slightly improved PCE (10.22%) [189]. In parallel, Zhou and coworkers synthesized **P30** that also showed enhanced light absorption in the visible-NIR range with a narrow bandgap of *ca* 1.42 eV and a high absorption coefficient of 6.85×10^4 cm^{-1} at 780 nm. All-PSCs prepared from the PBDB-T:**P30** photoactive blend were able to reach a PCE over 10% (10.7%) [190]. Further improvements were reported by Li and coworkers through the preparation of **P31**, consisting in copolymerizing the high efficient Y6 with a thiophene unit. Beyond promising PCEs (12.52%), the un-encapsulated devices exhibited long-term photostability over 300 h when placed in a nitrogen-filled glove box [191]. In 2020, the polymer **P32** was synthesized by Min and coworkers. **P32** was successfully embedded in OSCs with PM6, achieving PCEs of 13.44% [192]. Besides, enhancing the complementarity with the donor was found to significantly improve the efficiencies since blends of **P33** with PM6 achieved high PCE of 15.05% [193]. In 2022, Peng and coworkers reported the polymer **P34**. By adding a third component (PBDTCl-TPD) into a blend of PTQ10:**P34**, a maximum PCE of 16.04% was obtained in an All-PSCs [194]. The PCE was finally slightly improved by side chain engineering since Sun and coworkers developed a polymer (**P35**) that set a record with efficiency of 16.76% (16.3 certified%) [195].

The data of BT-based polymers for OSCs are listed in Table 3.

Table 2
Device parameters of BT-based acceptor molecules in OSCs.

	E_g^{opt}(eV)	HOMO/LUMO (eV)	V_{OC} (V)	J_{SC} (mA/cm^2)	FF (%)	PCE (%)	Donor	Ref.
A0	2.38	−5.87/−3.49	0.67	–	–	0.45	P3HT	[99]
A1	1.76	−5.38/−3.62	0.59	4.01	33	0.83	P3HT	[100]
A2	–	–	1.08	2.76	37	1.10	D2	[101]
A3	1.35	−5.06/−3.71	1.08	2.06	52	1.16	P3HT	[102]
A4	–	–	0.54	4.85	55	1.43	P3HT	[103]
A5	2.70	−6.01/−3.31	0.76	5.59	48	2.05	P3HT	[104]
A6	1.97	−5.62/−3.65	0.77	6.14	44	2.11	P3HT	[105]
A7	1.89	−5.99/−3.53	1.05	3.72	60	2.40	DPP-Py	[106]
A8	–	–	0.96	4.70	56	2.54	P3HT	[107]
A9	1.73	−6.01/−3.60	0.90	5.18	60	2.81	P3HT	[108]
A10	1.52	−5.85/−4.33	0.81	12.10	51	5.00	PTB7	[109]
A11	1.83	−5.76/−3.58	1.02	15.27	54	8.33	PTBT-Th	[110]
A12	1.45	−5.56/−3.89	0.82	17.06	65	9.13	PBDB-T	[111]
A13	1.54	−5.34/−3.87	0.87	18.59	65	10.52	PBDB-T	[112]
A14	1.37	−5.92/−4.23	0.80	20.57	70	11.48	PBDB-T	[113]
A15	1.47	−5.48/−3.97	0.86	19.80	67	11.50	J71	[114]
A16	1.72	−5.38/−3.66	0.74	25.93	60	11.62	PTB7-Th	[115]
A17	1.68	−5.55/−3.87	0.88	22.80	70	14.10	PBDB-T	[116]
A18	1.94	−5.56/−3.50	0.83	25.3	75	15.70	PM6	[18]
A19	–	–	0.89	24.24	72	16.50	PBDBT-TF	[119]
A20	–	−5.58/−3.84	0.83	24.82	70	14.94	–	[118]
A21	–	−5.48/−3.10	0.99	1.81	45	0.81	P3HT	[125]
A22	–	−5.48/−3.55	0.54	7.40	47	1.90	PBDB-T	[126]
A23	1.59	−5.26/−3.66	0.72	5.81	61	2.55	P3HT	[127]
A24	1.75	−5.41/−3.56	0.72	10.02	66	6.08	P3HT	[128]
A25	2.12	−5.89/−3.77	0.91	4.60	34	1.42	PTB7-Th	[129]
A26	2.07	−5.84/−3.77	1.00	8.10	40	3.30	PTB7-Th	[129]
A27	2.10	−5.78/−3.73	0.95	12.70	53	6.15	PffBT4T-2OD	[130]
A28	2.14	−5.70/−3.57	0.82	7.95	63	4.10	P3HT	[131]
A29	1.83	−5.39/−3.50	1.05	10.27	68	7.30	PBDB-T	[132]
A30	1.72	−5.44/−3.72	0.92	15.91	56	8.16	PTB7-Th	[133]
A31	–	−5.93/−3.86	0.93	17.86	74	12.27	PBDB-T	[135]
A32	2.11	−6.18/−3.67	0.88	11.20	51	5.00	PTB7-Th	[136]
A33	2.02	−6.10/−3.64	0.88	10.60	53	5.30	PTB7-Th	[136]
A34	1.45	−5.79/−3.90	0.66	11.90	60	5.00	PTB7-Th	[136]
A35	1.52	−5.30/−3.70	0.89	13.47	59	7.04	PBDB-T	[138]
A36	1.52	−5.30/−3.71	0.90	14.94	55	7.43	PBDB-T	[138]
A37	1.52	−5.30/−3.71	0.88	16.30	64	9.29	PBDB-T	[138]
A38	1.49	−5.28/−3.70	0.90	14.88	59	7.94	PBDB-T	[138]
A39	–	−5.69/−3.64	0.93	13.45	65	8.11	PBTA-BO	[140]
A40	–	–	0.99	9.4	56	5.30	PTzBI	[139]
A41	1.69	−5.30/−3.56	1.02	13.9	52	8.30	PTB7-Th	[141]
A42	1.63	−5.38/−3.67	0.88	12.9	52	5.70	PTB7-Th	[141]
A43	–	–	0.83	15.5	63	8.40	PTB7-Th	[142]
A44	–	−5.52/−3.69	1.04	14.7	65	10.10	PTB7-Th	[143]
A45	–	−5.28/−3.67	1.04	13.1	64	8.70	PTB7-Th	[144]
A46	–	−5.71/−3.77	0.91	14.52	67	9.06	PBTA-BO	[145]
A47	1.72	−5.67/−3.75	1.08	15.72	56	9.51	PTB7-Th	[146]
A48	2.19	−5.98/−3.71	0.95	13.75	64	8.29	PTB7-Th	[147]
A49	2.10	−5.95/−3.72	0.94	16.75	65	10.15	PTB7-Th	[147]
A50	–	–	1.02	17.2	63	11.10	PffBT4T-2DT	[148]
A51	1.40	−5.31/−3.89	0.81	17.58	48	7.05	PBDB-T	[149]
A52	1.39	−5.45/−3.90	0.80	20.29	60	10.18	PBDB-T	[149]

Table 3
Device parameters of BT-based polymers in OSCs.

	E_g^{opt}(eV)	HOMO/LUMO (eV)	V_{OC} (V)	J_{SC} (mA/cm^2)	FF (%)	PCE (%)	The other blend	Ref.
P1	1.6	–	0.68	–	33	0.34	PCBM	[165]
P2	2	–	0.33	0.25	30	0.02	PCBM	[166]
P3	1.98	–	1.4	4.66	46	2.41	PCBM	[167]
P4	1.4	−5.50/−3.60	0.65	11.8	46	3.50	PCBM	[168]
P5	1.8	−5.30/−3.55	0.85	8.98	47	3.59	P(NDI2OD-T2)	[169]
P6	1.88	−5.21/−3.35	0.89	6.92	64	3.60	PCBM	[170]
P7	1.95	−5.54/−3.33	1.07	6.29	55	3.71	NI-AA-NI	[171]
P8	1.45	−5.05/−3.27	0.68	12.7	55	5.10	PCBM	[172]
P9	1.95	−5.36/−3.74	0.81	9.6	69	5.40	PC71BM	[173]
P10	1.6	−5.20/−3.74	0.63	10.05	40	2.65	P(NDI2HD-T2)	[174]
P11	1.6	−5.77/−3.78	0.72	14.03	50	5.00	P(NDI2HD-T2)	[174]
P12	1.65	−5.14/−3.54	0.79	15.23	53	6.24	P(NDI2HD-T2)	[174]
P13	1.82	−5.50/−3.70	1.11	11.53	50	6.45	RR-PBN	[175]
P14	1.7	−5.28/−3.33	0.91	12.91	61	7.20	PC61BM	[176]
P15	1.78	−5.20/−3.60	0.95	4.4	27	1.55	ITIC	[177]

(*continued on next page*)

Table 3 (*continued*)

	E_g^{opt}(eV)	HOMO/LUMO (eV)	V_{OC} (V)	J_{SC} (mA/cm^2)	FF (%)	PCE (%)	The other blend	Ref.
P16	1.79	−5.26/−3.61	0.86	14.9	57	7.28	ITIC	[177]
P17	1.62	−5.27/−3.10	0.76	16.2	62	7.64	PC61BM	[178]
P18	1.38	−5.49/−3.70	0.68	17.8	65	7.90	PC71BM	[179]
P19	1.46	−5.26/−3.61	0.66	20.69	71	9.76	PC71BM	[180]
P20	1.63	−5.42/−3.52	1.08	14.32	67	10.40	O-IDTBR	[181]
P21	1.9	−5.46/−3.56	1.13	13.89	66	10.50	FTTB-PDI4	[182]
P22	1.81	−5.43/−3.58	0.91	17.3	71	11.00	IDIC	[183]
P23	1.58	−5.27/−3.65	0.73	23.74	70	12.10	IEICO-4F	[184]
P24	1.79	−5.30/−3.51	0.81	22.13	73	13.07	ZITI-N-EH	[185]
P25	1.98	−5.51/−2.77	0.86	27.7	77	20.27	Y6	[18]
P26	1.28	−5.37/−3.15	1.15	3.6	34	1.20	P3HT	[186]
P27	1.72	−5.63/−3.52	1.08	9.81	51	5.37	CD1	[187]
P28	1.43	−5.59/−3.75	0.53	14.2	65	8.32	PBDB-T	[188]
P29	1.28	−5.51/−3.87	0.7	22.52	65	10.22	PBDTTT-E-T	[189]
P30	1.42	−5.61/−3.80	0.92	18.27	64	10.70	PBDB-T	[190]
P31	1.82	−5.65/−3.83	0.9	21.33	65	12.52	PBDB-T	[191]
P32	1.77	−5.69/−3.92	0.93	21.78	66	13.44	PM6	[192]
P33	1.39	−5.68/−3.94	0.93	22.3	72	15.05	PM6	[193]
P34	1.95	−5.87/−3.92	0.89	23.91	75	16.04	PTQ10	[194]
P35	1.77	−5.60/−3.83	0.95	23.73	74	16.76	PM6	[195]

4. Conclusion

The aim of this review was thus to provide a general overview on the application of the BT building block for efficient OSC's donor and acceptor materials. Considering the large number of reported materials, it is unambiguous that BT is among the list of key building blocks to success and efficiency, particularly for the design of new generation of molecular NFAs. Through a fine tuning in molecular design, BT-based molecules have indeed achieved remarkable progress in OSCs, with PCE increasing from less than 2% to the current state of the art, *i.e.*, more than 18% with the Y6 family.

In general, the future development of BT-based materials for OSCs might be directing as following:

First, new BT-based units should definitively be continuously developed, using new design strategies or new molecular structures. However, the traditional trial-and-error development strategy must be discarded since it is highly time and resource consuming. Consequently new technologies should be massively exploited such as machine learning (ML) algorithms to generate combinations and simulate properties to anticipate a potential complementarity and compatibility with the active layer constituting counterpart. Numerous studies have already been reported demonstrating the *in situ* power of the method.

Secondly, another key factor to take into consideration would be the synthetic complexity of the target material. Most of the reported efficient materials indeed required numerous synthetic steps with an overall low synthetic yield. Hence, once again with the help of modern methods such as ML algorithms, the price and accessibility of starting materials should be strongly taken into consideration. For instance, beyond the scientific achievement, the polymerization of Y6 NFA raises questions on a potential industrialization of such materials.

Furthermore beyond achieving high PCE, stability of the devices should definitively attract more attention. Only several studies discuss this essential data but even if limited, some of them predict highly interesting and promising achievements. For instance, a decrease of the initial value to only 80% (T80), over 1000 h for lab NFA based OSCs under constant illumination was demonstrated, thus potentially achieving an exciting shelf-life of more than 10 years. Therefore, efforts must be clearly focused on improving device structures and encapsulation to meet the industrialization's prerequisites.

In conclusion, BT-based materials exhibit many promising properties in organic electronics and are key materials for OSCs. With efficiencies reaching 20%, simplification of their synthesis must now be the leading challenge for chemist as well as a proper device engineering to achieve high stability to, at last, move from academia to industry.

Declaration of competing interest

The authors declare that they have no known competing financial interests or personal relationships that could have appeared to influence the work reported in this paper.

Acknowledgments

Authors thank Jiangsu Nata Optoelectronic Material Co., Ltd. for support. The authors acknowledge financial support from Major Program of Natural Science Foundation of the Higher Education Institutions of Jiangsu Province, China (No. 19KJA460005) and Special Science and Technology Innovation Fund of Jiangsu Province on Carbon Peak and Carbon Neutralization-Frontier Fundamental Project (No. BK20220010).

References

[1] Y.H. Liu, B.W. Liu, C.Q. Ma, et al., Sci. China Chem. 65 (2021) 224–268.
[2] J.C. Zhang, S.F. Xie, X.J. Zhang, et al., Chem. Commun. 53 (2017) 537–540.
[3] S.S. Chen, G.Y. Zhang, J. Liu, et al., Adv. Mater. 29 (2017) 1604231.
[4] X.W. Zhu, B.Z. Xia, K. Lu, et al., Chem. Mater. 28 (2016) 943–950.
[5] Y. Zhou, K.L. Gu, X.D. Gu, et al., Chem. Mater. 28 (2016) 5037–5042.
[6] X.K. Liu, W.D. Xu, S. Bai, et al., Nat. Mater. 20 (2021) 10–21.
[7] Q.F. Ye, Y. Zhao, S.Q. Mu, et al., Adv. Mater. 31 (2019) 1905143.
[8] B.C. Yu, J.J. Shi, S. Tan, et al., Angew. Chem. Int. Ed. 60 (2021) 13436–13443.
[9] A. Renaud, P.Y. Jouan, N. Dumait, et al., ACS Appl. Mater. Interfaces 14 (2022) 1347–1354.
[10] Y. Xu, G.D. Li, R.S. Li, et al., Nano Energy 95 (2022) 106973.
[11] X.Y. Liu, H.J. Lian, Z.R. Zhou, et al., Adv. Energy Mater. 12 (2022) 2103933.
[12] D. Fang, Y. Tong, F.T. Xu, et al., J. Solid State Chem. 294 (2021) 121902.
[13] J.J. Yoo, G. Seo, M.R. Chua, et al., Nature 590 (2021) 587–593.
[14] X.P. Zheng, Y. Hou, C.X. Bao, et al., Nat. Energy 5 (2020) 131–140.
[15] J. Jeong, M. Kim, J. Seo, et al., Nature 592 (2021) 381–385.
[16] C. Zuo, H.J. Bolink, H. Han, et al., Adv. Sci. 3 (2016) 1500324.
[17] G. Kim, H. Min, K. Lee, Science 370 (2020) 108–112.
[18] Q.S. Liu, Y.F. Jiang, K. Jin, et al., Sci. Bull. 65 (2020) 272–275.
[19] Y. Cui, H.F. Yao, J.Q. Zhang, et al., Adv. Mater. 32 (2020) 1908205.
[20] L.L. Zhan, S.X. Li, T.K. Lau, et al., Energy Environ. Sci. 13 (2020) 635–645.
[21] L. Ye, M.Y. GaoJ, H. Hou, Sci. China Chem. 64 (2021) 1875–1887.
[22] Y.X. Du, H.T. Sheng, D. Astruc, M.Z. Zhu, Chem. Rev. 120 (2020) 526–622.
[23] S. Liu, J. Yuan, W.Y. Deng, et al., Nat. Photonics 14 (2020) 300–305.
[24] G.R. Chen, Y.Z. Li, M. Bick, J. Chen, Chem. Rev. 120 (2020) 3668–3720.
[25] D. Wang, Z.F. Yang, F. Liu, et al., Chin. Chem. Lett. 33 (2022) 466–469.
[26] M.V. Khenkin, E.A. Katz, A. Abate, et al., Nat. Energy 5 (2020) 35–49.

[27] C. Li, J.D. Zhou, J.L. Song, et al., Nat. Energy 6 (2021) 605–613.
[28] Q.Q. Li, Z. Li, Acc. Chem. Res. 53 (2020) 962–973.
[29] S.X. Li, C.Z. Li, M.M. Shi, H.Z. Chen, ACS Energy Lett. 5 (2020) 1554–1567.
[30] M. Zhang, L. Zhu, G.Q. Zhou, et al., Nat. Commun. 12 (2021) 309.
[31] M. Zhong, K. Tran, Y. Min, et al., Nature 581 (2020) 178–183.
[32] L. Zhu, M. Zhang, G.Q. Zhou, et al., Adv. Energy Mater. 10 (2020) 1904234.
[33] W.R. Xu, Y.L. Chang, X.W. Zhu, et al., Chin. Chem. Lett. 33 (2022) 123–132.
[34] H. Bronstein, C.B. Nielsen, B.C. SchroederI McCulloch, Nat. Rev. Chem. 4 (2020) 66–77.
[35] C.L. Li, H.L. Wang, F. Wang, et al., Light: Sci. Appl. 9 (2020) 31.
[36] Z. Zheng, J.Q. Wang, P.Q. Bi, et al., Joule 6 (2022) 171–184.
[37] G. Qing, R. Ghazfar, S.T. Jackowski, et al., Chem. Rev. 120 (2020) 5437–5516.
[38] X. Gao, K.B. Yu, Y.J. Zhao, et al., Chin. Chem. Lett. 33 (2022) 4659–4663.
[39] N.S. Sariciftci, L. Smilowitz, A.J. Heeger, Science 258 (1992) 1474–1476.
[40] D. Kearns, M. Calvin, J. Chem. Phys. 29 (1958) 950–951.
[41] C.W. Tang, Appl. Phys. Lett. 48 (1986) 183–185.
[42] G. Yu, J. Gao, J.C. Hummelen, F. WudlA, J. Heeger, Science 270 (1995) 1789–1791.
[43] Y.Z. Lin, J.Y. Wang, Z.G. Zhang, et al., Adv. Mater. 27 (2015) 1170–1174.
[44] W.C. Zhao, D.P. Qian, S.Q. Zhang, et al., Adv. Mater. 28 (2016) 4734–4739.
[45] L.X. Meng, Y.M. Zhang, X.J. Wan, Science 361 (2018) 1094–1098.
[46] J. Yuan, Y.Q. Zhang, L.Y. Zhou, et al., Joule 3 (2019) 1140–1151.
[47] R. Sun, Q. Wu, J. Guo, et al., Joule 4 (2020) 407–419.
[48] S. Akin, E. AkmanS Sonmezoglu, Adv. Funct. Mater. 30 (2020) 2002964.
[49] Y. Firdaus, V.M. Le Corre, S. Karuthedath, et al., Nat. Commun. 11 (2020) 5220.
[50] G.P. Kini, S.J. Jeon, D.K. Moon, Adv. Mater. 32 (2020) 1906175.
[51] D. Koo, S. Jung, J. Seo, et al., Joule 4 (2020) 1021–1034.
[52] C.Y. Liao, Y. Chen, C.C. Lee, et al., Joule 4 (2020) 189–206.
[53] W.C. Zhao, S.S. Li, H.F. Yao, et al., J. Am. Chem. Soc. 139 (2017) 7148–7151.
[54] Y. Cui, H.F. Yao, J.Q. Zhang, et al., Nat. Commun. 10 (2019) 2515.
[55] L. Hong, H.F. Yao, Z.A. Wu, et al., Adv. Mater. 31 (2019) 1903441.
[56] J.Y. Kim, J.W. Lee, H.S. Jung, H. ShinN, G. Park, Chem. Rev. 120 (2020) 7867–7918.
[57] R.X. Lin, K. Xiao, Z.Y. Qin, et al., Nat. Energy 4 (2019) 864–873.
[58] Y.B. Lin, B. Adilbekova, Y. Firdaus, et al., Adv. Mater. 31 (2019) 1902965.
[59] R. Wang, M. Mujahid, Y. Duan, et al., Adv. Funct. Mater. 29 (2019) 1808843.
[60] X.P. Xu, K. Feng, Z.Z. Bi, et al., Adv. Mater. 31 (2019) 1901872.
[61] T.T. Yan, W. Song, J.M. Huang, et al., Adv. Mater. 31 (2019) 1902210.
[62] F. Pan, X.J. Li, S. Bai, et al., Chin. Chem. Lett. 32 (2021) 1257–1262.
[63] Y. Cui, H.F. Yao, L. Hong, et al., Natl. Sci. Rev. 7 (2020) 1239–1246.
[64] J.J. Yoo, S. Wieghold, M.C. Sponseller, et al., Energy Environ. Sci. 12 (2019) 2192–2199.
[65] Q. Wang, S.Y. Lei, M. Luo, et al., ACS Appl. Mater. Interfaces 13 (2021) 36080–36088.
[66] M. Zhao, Y.X. Li, L. Liu, et al., Sol. Energy 224 (2021) 883–888.
[67] Y.Q. Zhang, X.F. Xu, J.R. Lu, S.M. Zhang, RSC Adv. 9 (2019) 14657–14661.
[68] S.M. Zhang, Y.L. Guo, Y.J. Zhang, et al., Chem. Commun. 46 (2010) 2841–2843.
[69] M.Y. Zhang, T.F. Li, G.H.J. Zheng, et al., Mater. Chem. Front. 1 (2017) 2078–2084.
[70] S.B. Shi, H. Wang, P. Chen, et al., Polym. Chem. 9 (2018) 3873–3884.
[71] S.M. Yu, Y.S. Chen, L. Yang, et al., J. Mater. Chem. A 5 (2017) 21674–21678.
[72] W.Y. Ye, Y. Yang, Z.Z. Zhang, et al., Sol. RRL 4 (2020) 2000258.
[73] F. Liu, T.Y. Hou, X.F. Xu, et al., Macromol. Rapid Commun. 39 (2018) 1700555.
[74] S. Song, J.R. Lu, W.Y. Ye, et al., Sci. China Chem. 64 (2021) 1441–1459.
[75] L.Y. Sun, X.F. Xu, S. Song, et al., Macromol. Rapid Commun. 40 (2019) 1900074.
[76] A. Khalid, R.A. Khera, A. Saeed, et al., Optik (Stuttg) 228 (2021) 166138.
[77] M.U. Khan, M.Y. Mehboob, R. Hussain, et al., Int. J. Quantum Chem. 120 (2020) 26377.
[78] A.P. Komin, R.W. Street, M. Carmack, J. Org. Chem. 40 (1975) 2749–2752.
[79] A.L. Jones, Z.L. Zheng, P. Riley, et al., Chem. Mater. 31 (2019) 9729–9741.
[80] Q.L. Nie, A.L. Tang, Q. Guo, E. Zhou, Nano Energy 87 (2021) 106174.
[81] Z.F. Zang, Q.G. Wang, P. Song, F.C. Ma, Y.Z. Li, Sol. Energy 231 (2022) 503–515.
[82] N.B. A.lmandil, M. Taha, F. Rahim, et al., Bioorg. Chem. 85 (2019) 109–116.
[83] C. Brillada, O.K. Teh, F.A. Ditengou, et al., Plant Cell 33 (2021) 404–419.
[84] B. Chen, N. Yang, P. Wang, Y.G. Xiang, H. Chen, Appl. Surf. Sci. 499 (2020) 143865.
[85] J.H. Jia, T. Li, Y.H. Cui, et al., Dyes Pigments 162 (2019) 26–35.
[86] W.H. Zeng, L.Y. Wu, Y.D. Sun, et al., Small 17 (2021) 2101924.
[87] X.H. Zhang, J. Xiao, C. Peng, Y.G. Xiang, H. Chen, Appl. Surf. Sci. 465 (2019) 288–296.
[88] Z.F. Zhao, Y.L. Zheng, C. Wang, et al., ACS Catal. 11 (2021) 2098–2107.
[89] W.W. Li, C. Du, F.H. Li, et al., Chem. Mater. 21 (2009) 5327–5334.
[90] Y. Yang, J. Zhang, Y. Zhou, J. Phys. Chem. C 114 (2010) 3701–3706.
[91] J.J. Chen, T.L. Chen, B. Kim, et al., ACS Appl. Mater. Interfaces 2 (2010) 2679–2686.
[92] P. Dutta, J. Kim, S.H. Eom, et al., ACS Appl. Mater. Interfaces 4 (2012) 6669–6675.
[93] L.Y. Lin, C.W. Lu, W.C. Huang, et al., Org. Lett. 13 (2011) 4962–4965.
[94] Y. Jeon, T.M. Kim, J.J. Kim, J.I. Hong, New J. Chem. 39 (2015) 9591–9595.
[95] Q. Shang, M. Wang, J.J. Wei, Q.D. Zheng, RSC Adv. 7 (2017) 18144–18150.
[96] T.S. van der Poll, J.A. Love, T.Q. Nguyen, G.C. Bazan, Adv. Mater. 24 (2012) 3646–3649.
[97] Y.H. Chen, L.Y. Lin, C.W. Lu, et al., J. Am. Chem. Soc. 134 (2012) 13616–13623.
[98] W.C. Wang, G.J. Zhang, J.L. Guo, et al., ACS Appl. Energy Mater. 2 (2019) 4730–4736.
[99] R.Y.C. Shin, T. Kietzke, S. Sudhakar, Chem. Mater. 19 (2007) 1892–1894.
[100] S. Somasundaram, S. Jeon, S. Park, Macromol. Res. 24 (2016) 226–234.
[101] B. Walker, X. Han, C. Kim, A. Sellinger, T.Q. Nguyen, ACS Appl. Mater. Interfaces 4 (2012) 244–250.
[102] A.M. Raynor, A. Gupta, H. Patil, A. Bilic, S.V. Bhosale, RSC Adv. 4 (2014) 57635–57638.
[103] Y. Fang, A.K. Pandey, A.M. Nardes, et al., Adv. Energy Mater. 3 (2013) 54–59.
[104] S. Jinnai, Y. Ie, M. Karakawa, et al., Chem. Mater. 28 (2016) 1705–1713.
[105] L.Y. Lan, B.F. Zhao, J. Zhang, et al., New J. Chem. 43 (2019) 3565–3571.
[106] J.D. Douglas, M.S. Chen, J.R. Niskala, et al., Adv. Mater. 26 (2014) 4313–4319.
[107] J.T. Bloking, X. Han, A.T. Higgs, et al., Chem. Mater. 23 (2011) 5484–5490.
[108] S. Chatterjee, Y. Ie, M. KarakawaY Aso, Adv. Funct. Mater. 26 (2016) 1161–1168.
[109] J.W. Jung, W.H. Jo, Chem. Mater. 27 (2015) 6038–6043.
[110] T. Lee, C.E. Song, S.K. Lee, W.S. ShinE Lim, ACS Omega 6 (2021) 4562–4573.
[111] H.S. Kim, C.E. Song, J.W. Ha, et al., ACS Appl. Mater. Interfaces 11 (2019) 47121–47130.
[112] M. Zhang, M. Zeng, H.J. Chen, et al., Sol. Energy 197 (2020) 511–518.
[113] Y.Z. Wang, Z.W. Liu, X.Y. Cui, et al., J. Mater. Chem. A 8 (2020) 12495–12501.
[114] G.L. Cai, Y.H. Li, J.Y. Wang, et al., ACS Appl. Polym. Mater. 3 (2020) 23–29.
[115] D. Luo, M. Zhang, J.B. Li, et al., J. Mater. Chem. C 8 (2020) 6196–6202.
[116] J. Yuan, Y.Q. Zhang, L.Y. Zhou, et al., Adv. Mater. 31 (2019) 1807577.
[117] L. Perdigon-Toro, H.T. Zhang, A. Markina, et al., Adv. Mater. 32 (2020) 1906763.
[118] H. Yu, Z.Y. Qi, J.Q. Zhang, et al., J. Mater. Chem. C 8 (2020) 23756–23765.
[119] J. Yuan, H.T. Zhang, R. Zhang, et al., Chem 6 (2020) 2147–2161.
[120] Q.Y. Wei, W. Liu, M. Leclerc, et al., Sci. China Chem. 63 (2020) 1352–1366.
[121] H. Yu, Z.Y. Qi, X.Y. Li, et al., Sol. RRL 4 (2020) 2000421.
[122] P. Gopikrishna, H. Choi, D.H. Kim, et al., Chem. Sci. 12 (2021) 14083–14097.
[123] X.F. Li, M.A. Pan, T.K. Lau, et al., Chem. Mater. 32 (2020) 5182–5191.
[124] D.Q. Hu, Q.G. Yang, Y.J. Zheng, et al., Adv. Sci. 8 (2021) 2004262.
[125] Y.Z. Lin, H.F. Wang, Y.F. Li, D.B. Zhu, X.W. Zhan, J. Mater. Chem. A 1 (2013) 14627–14632.
[126] Y.T. Guo, A.D. Zhang, C. Li, W.W. Li, D.B. Zhu, Chin. Chem. Lett. 29 (2018) 371–373.
[127] B. Xiao, A.L. Tang, Q.Q. Zhang, et al., ACS Appl. Mater. Interfaces 10 (2018) 34427–34434.
[128] B. Xiao, A.L. Tang, L.X. Cheng, et al., Sol. RRL 1 (2017) 1700166.
[129] C.L. Radford, A.D. Hendsbee, M. Abdelsamie, et al., ACS Appl. Energy Mater. 1 (2018) 6513–6523.
[130] H. Tan, Y. Long, J. Zhang, et al., Dyes Pigments 162 (2019) 797–801.
[131] S. Holliday, R.S. Ashraf, C.B. Nielsen, et al., J. Am. Chem. Soc. 137 (2015) 898–904.
[132] J. Zhang, J. Lv, X.Y. Dong, et al., J. Mater. Chem. C 8 (2020) 9195–9200.
[133] C.Q. Tang, S.C. Chen, Y.B. Tang, W. Ma, Q. Zheng, Sol. Energy 174 (2018) 991–998.
[134] F. Liu, Y. Gu, C. Wang, et al., Adv. Mater. 24 (2012) 3947–3951.
[135] X.P. Xu, Z.Z. Bi, W. Ma, et al., Adv. Mater. 29 (2017) 1704271.
[136] K. Wang, Y. Firdaus, M. Babics, et al., Chem. Mater. 28 (2016) 2200–2208.
[137] S. Holliday, R.S. Ashraf, A. Wadsworth, et al., Nat. Commun. 7 (2016) 11585.
[138] J.F. Qu, Z. Mu, H.J. Lai, et al., ACS Appl. Energy Mater. 1 (2018) 4724–4730.
[139] W.K. Zhong, B.B. Fan, J. Cui, et al., ACS Appl. Mater. Interfaces 9 (2017) 37087–37093.
[140] B.B. Fan, W.K. Zhong, X.F. Jiang, et al., Adv. Energy Mater. 7 (2017) 1602127.
[141] Q.Y. Li, J.Y. Xiao, L.M. Tang, et al., Org. Electron. 44 (2017) 217–224.
[142] M.A. Alamoudi, J.I. Khan, Y. Firdaus, et al., ACS Energy Lett. 3 (2018) 802–811.
[143] P. Cheng, M.Y. Zhang, T.K. Lau, et al., Adv. Mater. 29 (2017) 1605216.
[144] W.Y. Bai, X.P. Xu, Q.Y. Li, Y.X. Xu, Q. Peng, Small Methods 2 (2018) 1700373.
[145] W.K. Zhong, J. Cui, B.B. Fan, et al., Chem. Mater. 29 (2017) 8177–8186.
[146] Y.L. Ma, M.Q. Zhang, Y.B. Tang, W. Ma, Q. Zheng, Chem. Mater. 29 (2017) 9775–9785.
[147] W.L. Wu, G.J. Zhang, X.P. Xu, et al., Adv. Funct. Mater. 28 (2018) 1707493.
[148] A. Wadsworth, R.S. Ashraf, M. Abdelsamie, et al., ACS Energy Lett. 2 (2017) 1494–1500.
[149] Y. Cui, P. Zhu, X. Xia, et al., Chin. Chem. Lett. 34 (2023) 107902.
[150] F. Pereira, K. Xiao, D.A. Latino, et al., J. Chem. Inf. Model. 57 (2017) 11–21.
[151] A. Mahmood, J.L. Wang, Energy Environ. Sci. 14 (2021) 90–105.
[152] G. Montavon, M. Rupp, V. Gobre, et al., New J. Phys. 15 (2013) 095003.
[153] H.C. Shi, W.Z. Jing, W. Liu, et al., ACS Omega 7 (2022) 7893–7900.
[154] S. Li, B.S.S. Pokuri, S.M. Ryno, et al., J. Chem. Inf. Model. 60 (2020) 1424–1431.
[155] B.S.S. Pokuri, S. Ghosal, A. Kokate, S. Sarkar, B. Ganapathysubramanian, NPJ Comput. Mater. 5 (2019) 95.
[156] M.Y. Sui, Z.R. Yang, Y. Geng, et al., Sol. RRL 3 (2019) 1900258.
[157] N. Majeed, M. Saladina, M. Krompiec, et al., Adv. Funct. Mater. 30 (2019) 1907259.
[158] X. Xu, J.Y. Xiao, G.C. Zhang, et al., Sci. Bull. 65 (2020) 208–216.
[159] J. Peet, J.Y. Kim, N.E. Coates, et al., Nat. Mater. 6 (2007) 497–500.
[160] Y.F. Li, Acc. Chem. Res. 45 (2012) 723–733.
[161] J. Bouffard, T.M. Swager, Macromolecules 41 (2008) 5559–5562.
[162] H.W. Hu, P.C.Y. Chow, G.Y. Zhang, et al., Acc. Chem. Res. 50 (2017) 2519–2528.
[163] Y. He, Q.L. Wang, X. Jing, et al., Org. Electron. 101 (2022) 106424.
[164] S.Y. Feng, H. Lu, Z.K. Liu, et al., Acta Physico-Chim. Sin. 35 (2019) 355–360.
[165] A. Dhanabalan, J.K.J. van Duren, P.A. van Hal, J.L.J. van Dongen, R.A.J. Janssen, Adv. Funct. Mater. 11 (2001) 255–262.
[166] E. BundgaardF, C. Krebs, Polym. Bull. 55 (2005) 157–164.
[167] M. Svensson, F.L. Zhang, S.C. Veenstra, et al., Adv. Mater. 15 (2003) 988–991.
[168] Z.G. Zhu, D. Waller, R. Gaudiana, Macromolecules 40 (2007) 1981–1986.
[169] H. Kang, M.A. Uddin, C. Lee, et al., J. Am. Chem. Soc. 137 (2015) 2359–2365.

[170] N. Blouin, A. MichaudM Leclerc, Adv. Mater. 19 (2007) 2295–2300.
[171] J. Zhang, X.J. Zhang, G.W. Li, et al., Chem. Commun. 52 (2016) 469–472.
[172] J.H. Hou, H.Y. Chen, S.Q. Zhang, G. Li, Y. Yang, J. Am. Chem. Soc. 130 (2008) 16144–16145.
[173] R.P. Qin, W.W. Li, C.H. Li, J. Am. Chem. Soc. 131 (2009) 14612–14613.
[174] K. Kranthiraja, S. Kim, C. Lee, et al., Adv. Funct. Mater. 27 (2017) 1701256.
[175] N. Wang, S. Zhang, R.Y. Zhao, et al., ACS Appl. Electron. Mater. 2 (2020) 2274–2281.
[176] H.X. Zhou, L.Q. Yang, A.C. Stuart, et al., Angew. Chem. Int. Ed. 50 (2011) 2995–2998.
[177] X. Gong, G.W. Li, S.Y. Feng, et al., J. Mater. Chem. C 5 (2017) 937–942.
[178] Z.H. Chen, P. Cai, J.W. Chen, et al., Adv. Mater. 26 (2014) 2586–2591.
[179] J.B. You, L.T. Dou, K. Yoshimura, et al., Nat. Commun. 4 (2013) 1446.
[180] S.B. Shi, Q.G. Liao, Y.M. Tang, et al., Adv. Mater. 28 (2016) 9969–9977.
[181] S.S. Chen, Y.M. Wang, L. Zhang, et al., Adv. Mater. 30 (2018) 1804215.
[182] J.Q. Zhang, Y.K. Li, J.C. Huang, et al., J. Am. Chem. Soc. 139 (2017) 16092–16095.
[183] Y.Z. Lin, F.W. Zhao, Y. Wu, et al., Adv. Mater. 29 (2017) 1604155.
[184] Z.M. Chen, Z.C. Hu, Y.Y. Liang, et al., Org. Electron. 85 (2020) 105874.
[185] J.Y. Zhang, W.R. Liu, M. Zhang, et al., J. Mater. Chem. A 8 (2020) 8661–8668.
[186] C.R. McNeill, J.J.M. Halls, R. Wilson, et al., Adv. Funct. Mater. 18 (2008) 2309–2321.
[187] Y.J. Yu, L. Zhang, J. Liu, L.X. Wang, Polymer 242 (2022) 124547.
[188] S.B. Shi, P. Chen, Y. Chen, et al., Adv. Mater. 31 (2019) 1905161.
[189] K. Feng, J.C. Huang, X.H. Zhang, et al., Adv. Mater. 32 (2020) 2001476.
[190] A.L. Tang, J.F. Li, B. Zhang, J. Peng, E. Zhou, ACS Macro. Lett. 9 (2020) 706–712.
[191] J. Du, K. Hu, L. Meng, et al., Angew. Chem. Int. Ed. 59 (2020) 15181–15185.
[192] W. Wang, Q. Wu, R. Sun, et al., Joule 4 (2020) 1070–1086.
[193] Z.H. Luo, T. Liu, R.J. Ma, et al., Adv. Mater. 32 (2020) 2005942.
[194] C.T. Liao, Y.F. Gong, X.P. Xu, et al., Chem. Eng. J. 435 (2022) 134862.
[195] Y. Li, J.L. Song, Y.C. Dong, et al., Adv. Mater. 34 (2022) 2110155.